



 Cite this: *RSC Adv.*, 2023, 13, 32904

# Enhancing drilling mud performance through CMITS-modified formulations: rheological insights and performance optimization

 Imtiaz Ali, <sup>\*ab</sup> Maqsood Ahmad,<sup>c</sup> Syahrir Ridha,<sup>d</sup> Cajetan Chimezie Iferobia<sup>a</sup> and Najeebullah Lashari<sup>e</sup>

In the context of deep well drilling, the addition of functionalized additives into mud systems becomes imperative due to the adverse impact of elevated borehole temperatures and salts on conventional additives, causing them to compromise their intrinsic functionalities. Numerous biomaterials have undergone modifications and have been evaluated in drilling muds. However, the addition of dually modified tapioca starch in bentonite-free mud systems remains a notable gap within the existing literature. This study aims to examine the performance of dually modified carboxymethyl irradiated tapioca starch (CMITS) under high temperature and salt-containing conditions employing central composite design approach; the study evaluates the modified starch's impact on mud rheology, thermal stability, and salt resistance. The findings indicated that higher DS (0.66) and CMITS concentrations (8 ppb) improved plastic viscosity (PV), yield point (YP) and gel strength (GS), while increased salt and temperature decreased it, demonstrating the complex interplay of these factors on mud rheology. The developed empirical models suggested that DS 0.66 starch addition enhanced rheology, especially at elevated temperatures, demonstrating improved borehole cleaning potential, supported by quadratic model performance indicators in line with American Petroleum Institute (API) ranges. The optimized samples showed a non-Newtonian behavior, and Power-law model fitting yields promising results for improved cuttings transportation with starch additives.

 Received 4th September 2023  
 Accepted 27th October 2023

DOI: 10.1039/d3ra06008j

[rsc.li/rsc-advances](http://rsc.li/rsc-advances)

## Introduction

With the increasing demand for fossil fuels and the decrease in the production rate in existing fields, more deep wells must be drilled to fulfil society's energy demand. The existence of high temperatures and pressures in such deep formations demand high-performance mud systems to drill a well successfully.<sup>1</sup> Moreover, the environmental concerns regarding the conventional chemicals used to improve the mud properties are important. Green and sustainable additives could be introduced in the oil industry which would reduce the cost and detrimental effects on the environment.<sup>2</sup>

In the past decades, mud's suspension capabilities and fluid loss control properties have been an industry research focus.

Numerous solutions have been suggested to enhance mud properties, particularly mud rheology, for successful drilling operation. It is considered one of the crucial parameters that leads to completing a well in an efficient way.<sup>3-5</sup> With the increase in downhole temperature, the conventional mud additives including biopolymers and cellulose derivatives degrade, resulting in the deterioration of mud properties.<sup>6,7</sup> In order to address these identified limitations, investigations are currently in progress aimed at identifying substitute materials *in lieu* of the conventional mud additives.

In recent years, non-damaging bentonite-free water-based muds have been used widely due to their better performance.<sup>8</sup> The main additives for regulating rheological and filtration properties of non-damaging muds are comprised primarily of acid-soluble resources, such as biopolymers, cellulose, inhibitors, and calcium carbonate. Such polymeric materials are proven to enhance viscosity and gel strength even at low concentrations. The starches, which are commonly used as rheology modifiers and fluid loss control agents, possess lower thermal stability and thus lose their basic functions when exposed to high-temperature conditions.<sup>9</sup> Thermal degradation of starch and cold-water solubility are the costly pitfalls of drilling operations, which lead to further operational problems, including fluid loss, barite sagging, drilling interruptions,

<sup>a</sup>Department of Petroleum Engineering, Universiti Teknologi PETRONAS, Seri Iskandar, 32610, Perak, Malaysia. E-mail: [imtiaz\\_17003333@utp.edu.my](mailto:imtiaz_17003333@utp.edu.my)

<sup>b</sup>Department of Petroleum and Gas Engineering, BUTEMS, Pakistan

<sup>c</sup>Department of Geosciences, Universiti Teknologi PETRONAS, Seri Iskandar, 32610, Perak, Malaysia

<sup>d</sup>Institute of Hydrocarbon Recovery, Universiti Teknologi PETRONAS, Seri Iskandar, 32610, Perak, Malaysia

<sup>e</sup>Department of Petroleum and Gas Engineering, Dawood University of Engineering & Technology, M. A. Jinnah Road, Karachi, 74800, Pakistan



formation damage, and pipe sticking.<sup>10–12</sup> Literature studies showed that starch polymers lose their primary functions after 249.8 °F.<sup>13</sup> It is important to maintain the stability of non-damaging muds' rheological characteristics at high temperatures.<sup>14,15</sup> In addition, the existence of excessive salts at the subsurface also impairs the rheological properties of mud containing starch and other biopolymers. The salt resistance has a detrimental influence on the mud's rheology, which ultimately lowers the mud's filtration characteristics and leads to higher fluid loss into the formation. Recent research reported that cross-linking and etherification are the better starch modification approaches for thermal stability enhancement without affecting its eco-friendly nature. In addition, when the carboxymethyl functional group is added to starch, its bacterial resistance also increases.<sup>15–17</sup>

Several researchers have emphasized the significance of modified starches,<sup>18–22</sup> cellulose derivatives,<sup>7,23,24</sup> and native biomaterials<sup>25,26</sup> for enhancing the rheological properties of mud. Nevertheless, there remains a necessity to enhance the temperature and salt resistance characteristics of these muds, particularly for their application in deep well drilling. Therefore, further investigation is required to explore and reveal advancements in material structures for potential utilization in drilling fluids.

The latest literature emphasizes the requirement for high-performance mud systems in drilling deep wells to meet growing energy demands while emphasizing environmental concerns linked to conventional chemicals. The challenges of temperature and salt resistance in starch-containing muds are identified, but there's a need for detailed insights into existing solutions and potential research gaps. In addition, the application of etherified starch in water-based muds is mentioned, but its rheological behavior in this context is not explored, constituting a gap in the understanding of its performance. Gamma irradiation is introduced as an environmentally friendly process for modifying starch, additional information on its applications and limitations in the oil industry is lacking. Therefore, a more in-depth analysis of existing technologies, recent research, and specific gaps in mud rheology, environmental sustainability, and modified starch applications is essential for a comprehensive understanding and further advancements in drilling fluid technologies.

The current work is an extension of our previous research,<sup>27</sup> which is focused on the utilization of the dually modified tapioca starch in water based drilling muds. The performance of the modified starch has been assessed in terms of mud rheological characteristics using central composite design approach. The thermal and salt resistance capabilities have also been investigated in this work. Finally, four empirical correlations have been developed and the models were validated and optimized through further experiments.

## Materials and methods

### Materials

In housed dually modified carboxymethyl starch with various degrees of substitution (DS: 0.56, 0.64 and 0.66) have been used. Premium-grade xanthan gum (XG), and polyanionic cellulose

(PAC) were precured from Scomi Oiltools and have been used without further process. Calcium carbonate, sodium hydroxide (NaOH), and salt (sodium chloride) were purchased from A&M.

### Experimental design

Design expert is a statistical software package that provides powerful tools to plan an ideal experiment on a process, mixture, or combination of factors and components. The graphical tools can aid in identifying the impact of each factor on the desired responses and reveal abnormalities in the data. In the current work, response surface methodology (RSM) was applied, which is a user-friendly statistical tool for designing, analyzing, optimizing, and validating experimental findings.<sup>28</sup> The current design used the RSM based on the central composite design (CCD) to obtain the mathematical correlation between selected factors and responses describing factors' interactions. Four parameters were considered as factors, including the starch degree of substitution (0.56, 0.64 and 0.66), starch dosage (0–8 ppb), salt concentration (0–6 M NaCl), and temperature (70–300 °F). The DS values were selected based on the three highest values obtained from carboxymethylation. In addition, plastic viscosity (PV), yield point (YP), and gel strength (both 10 s and 10 min) were selected as responses. The flow-chart of RSM is given in Fig. 1. The levels of factors and the corresponding codes of different independent variables are shown in Table 1.

The process performance was assessed by evaluating the responses based on the input factors  $X_1, X_2, \dots, X_n$ . The general relation between response parameters and input process parameters is described by eqn (1):

$$Y = f(X_1, X_2, X_3, \dots, X_n) + \text{error} \quad (1)$$

where  $f$  represents the actual response function and error describes the differentiation.

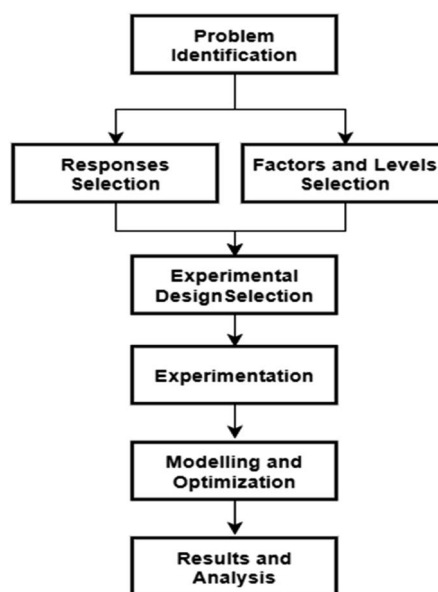


Fig. 1 Experimental design flowchart.



Table 1 Factor's design and corresponding codes

Factor	Units	Codes	Levels			
			Low	High	−alpha	+alpha
Degree of substitution	—	X <sub>1</sub>	0.56	0.66	0.56	0.66
CMITS concentration	ppb	X <sub>2</sub>	0	8	0	8
Salt concentration	ppb	X <sub>3</sub>	0	6	0	6
Temperature	°F	X <sub>4</sub>	70	300	70	300

In order to predict optimum conditions, the quadratic equation model of the response  $Y$  derived is a function of the levels of independent variables represented according to eqn (2). It is a second-order polynomial equation model for predicting the optimum point between factors and responses.<sup>29</sup>

$$Y = \beta_0 + \sum_{i=1}^k \beta_i x_i + \sum_{i=1}^k \beta_{ii} x_i^2 + \sum_{i=1}^k \sum_{j=i+1}^k \beta_{ij} x_i x_j + \dots e \quad (2)$$

where  $\beta$  is the regression coefficient,  $i$  and  $j$  are the linear and quadratic coefficients, respectively,  $k$  represents the number of examined factors optimized by the experiment while  $e$  represents the random error.<sup>30</sup>

Design expert was used for empirical model development, optimization, and confirmation of the models. The optimization module searches for a combination of factor levels that simultaneously satisfy the criteria placed on each of the responses and factors. It uses the models to search the factor space for the best trade-offs to achieve multiple goals.

### Mud preparation

All the mud blends were prepared considering the standard procedure defined by API. Initially, the multimixer cup was cleaned and filled with 350 mL of deionized water, with a pH maintained at 9.0–9.5 by adding sodium hydroxide. Xanthan gum was then added to the water at a concentration of 1.5 ppb. It was mixed for 30 minutes at 11 500 RPM using Fann Multimixer (Fann Model 9B) to ensure a homogenous mixture while intermittently dislodging any clinging to the wall of the mixing cup. Fluid loss control agents, including polyanionic cellulose (2 ppb) and modified starch (defined by DOE), were added to the mixture. Sodium chloride was added according to the DOE, and finally, 120 ppb of sized calcium carbonate was added to the mixture to achieve the required mud weight. The mixture was again mixed for 20 minutes. The base mud was composed of all the mentioned additives except CMITS.

### Performance evaluation

Several experimental equipment was used to evaluate the potential of modified starch for drilling fluid applications. The main apparatuses used in this experimental study include a rheometer (Discovery HR-1 TA Instruments, USA), viscometer (Fann 35A), and hot roll oven (Fann Model: 705ET). Mud samples were subjected under a wide range of shear rates (0.01–1200 s<sup>−1</sup>). The concentric cylindrical geometry was used for testing the muds, as such geometries are generally used for low

viscosity fluids.<sup>31</sup> The obtained data were examined by fitting the experimental data with the three frequently used models, including Bingham plastic, Power law, and Harshal Bulkley models to understand the best-fitted model for the selected mud samples.

Drilling fluid viscosity was measured using the API rotary viscometer. It is an industrial API recommended viscometer with coaxial cylinders. The fluid was placed between a rotor (sleeve) and a bob (solid cone). During rheology measurements, the viscous drag force applied by the fluid causes a torque on the bob, and a transducer evaluates the bob's deflection. According to American Petroleum Institute (API) standards, the mud rheological performance was measured in terms of plastic viscosity, yield point, and gel strength. The formulated mud sample was placed in the annular space between two concentric cylinders, and a steady rotational velocity was applied. Each experimental run was repeated three times to confirm its repeatability.

To mimic the reservoir conditions, the samples were subjected to high temperature in hot roll oven for 16 hours. Later, the mud rheology was measured to understand the influence of high temperature on the mud rheology.

## Results and discussion

### Effect on mud rheological properties

Various parameters significantly influence the mud's rheological properties, including the degree of substitution (DS), CMITS concentration, salt concentration, and temperature. The following sections discuss three mud rheological properties, including plastic viscosity, yield point, and gel strength (10 s and 10 min).

### Plastic viscosity

The influence of both degrees of substitution and CMITS concentration of the CMITS (DS 0.66) starch on the plastic viscosity of the mud is assessed and shown in Fig. 2(a). It can be observed that the increase in DS value also enhanced the plastic viscosity of the mud. The base mud showed a PV value of 16 cP. Considering the maximum CMITS concentration at 8 ppb, and salt concentration at 0 ppb at 70 °F, the PV for DS 0.56, 0.64 and 0.66, was 22, 27 and 29 cP, respectively. This increase corresponds to 47 and 80, and 93% increase when compared with the sample without starch. The findings show a direct relationship between CMITS dosage and the PV.

The sample without CMITS depicted the lowest PV because the given viscosity is due to the presence of xanthan gum and PAC, which supported the other mud additives to form a viscous mud. In contrast, the mud viscosity was increased due to the addition of high DS CMITS, where more carboxyl groups are attached to the starch. The carboxymethyl group concentration in modified starch molecules increased with increasing its degree of substitution (DS), resulting in the carboxymethyl group's hydrophilic characteristics, which further aids CMITS molecules in dissolving and extending in solution. It is known that biopolymers improve the rheology of mud due to the



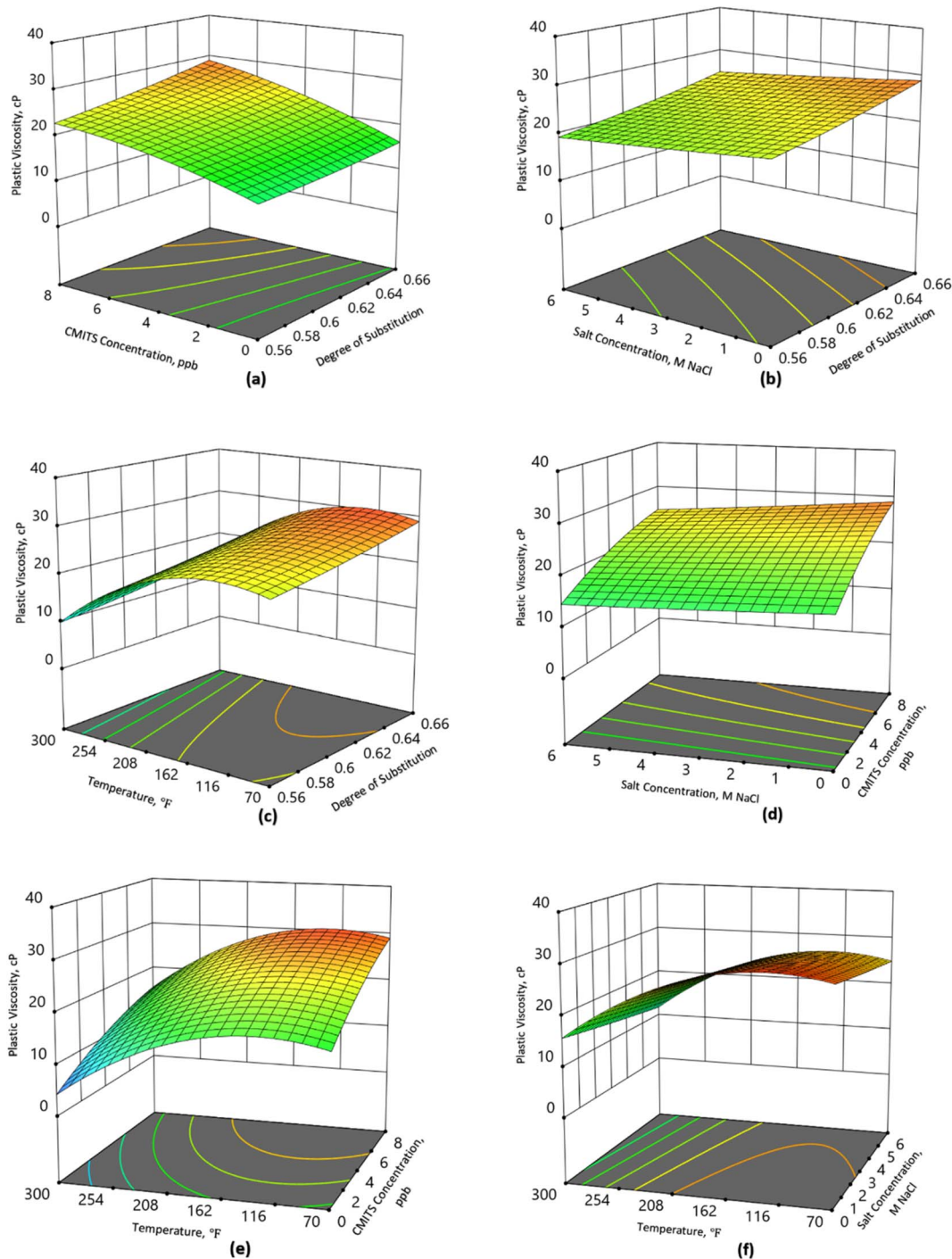


Fig. 2 Influence of (a) DS and CMITS dosage, (b) DS and salt dosage, (c) DS and temperature, (d) CMITS and salt dosage, (e) CMITS dosage and temperature, and (f) salt dosage and temperature on the plastic viscosity.

absorption and development of solvation shells, and these were further increased in the carboxymethylation.

Fig. 2(b) shows the combined effect of salt and CMITS concentration on the PV. The mud without salt showed better performance in terms of rheology. However, a downward shift in the PV was observed when the salt concentration was increased. The PV at zero salt concentration and maximum salt concentration (6 M NaCl) was 29 and 25 cP for the highest DS

starch, which showed a decrease of 14% at 70 °F. Compared with the DS 0.56, the PV was reduced from 23 to 19 cP, which is 17% decrease. The findings showed that the increase in salt content in the mud declines the viscosity, and a higher effect can be observed at the lower DS. This decline is attributed to the salt electrolyte weakening of the intramolecular ionic bonding, causing the molecular chain conformation to shift from curly spherical to flexible. With the rising electrolyte content of



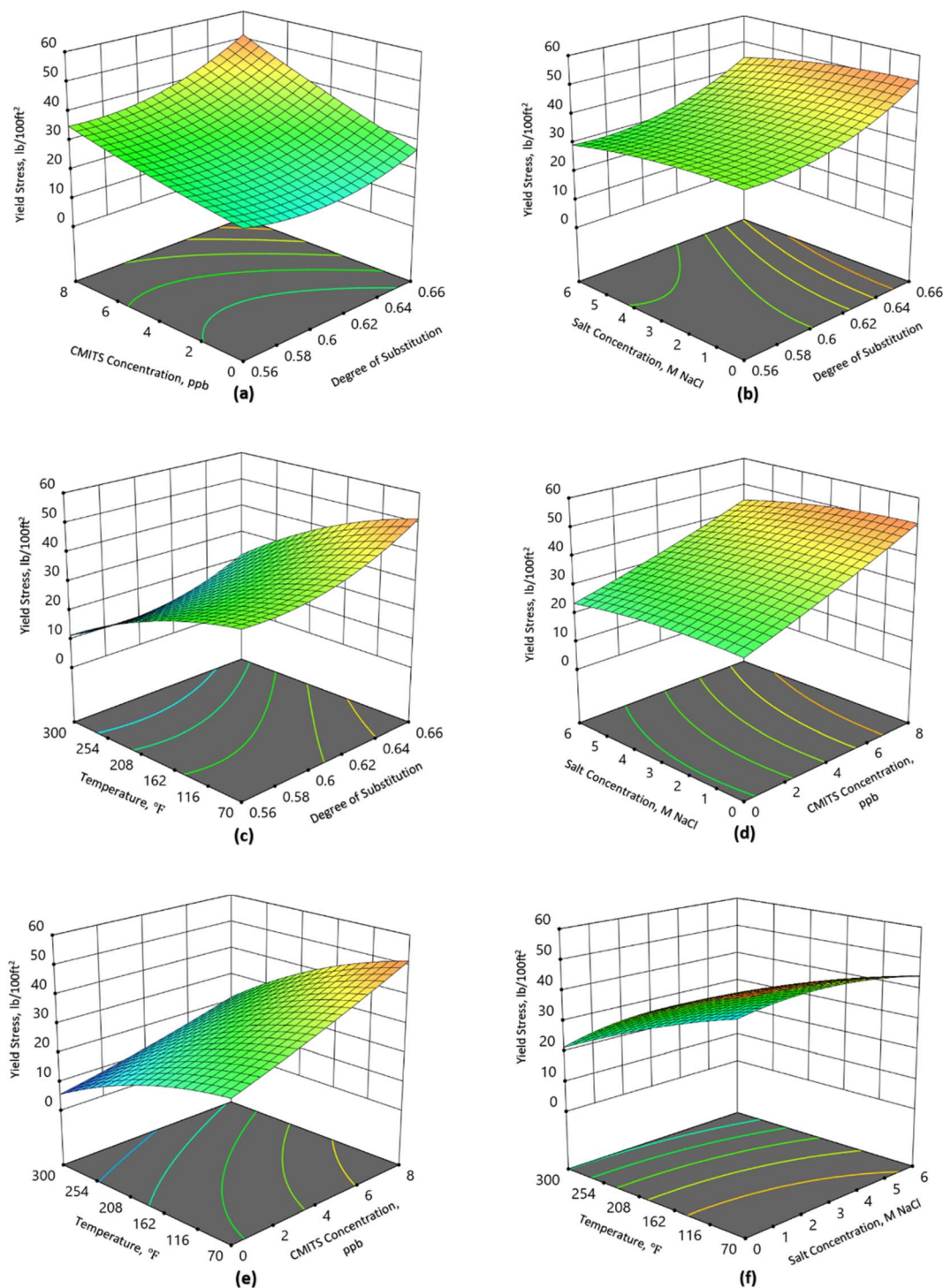


Fig. 3 Influence of (a) DS and CMITS dosage, (b) DS and salt dosage, (c) DS and temperature, (d) CMITS and salt dosage, (e) CMITS dosage and temperature, and (f) salt dosage and temperature on the yield point.

sodium chloride, this effect became more severe in the presence of high temperatures.

The performance of the CMITS in the presence of higher temperatures is shown in Fig. 2(c). It is revealed that for CMITS 0.56, the PV declined from 22 to 9 cP when the temperature was increased from 70 to 300 °F. This is a 59% reduction. While under the same conditions, the DS 0.66 showed reduced PV

from 29 to 16 cP, corresponding to a 45% decrease. The findings show that higher DS starch can sustain in a high-temperature environment. Although the PV of all the CMITS-based mud samples progressively declined as the NaCl concentrations increased, but the higher degree of substitution starch showed enhanced performance.



Fig. 2(d) shows the influence of salt and CMITS concentration. It is observed that the base fluid showed 16 cP plastic viscosity without salt concentration. When the salt concentration was increased to 6 M NaCl, the PV was reduced to 14. On the other hand, the PV of the CMITS 0.66 increased to 29 cP at 8 ppb concentration. Similarly, at the highest salt concentration (6 M NaCl), the PV of the 8 ppb CMITS starch was recorded as 25 cP. These findings demonstrated that CMITS-based fluids were salt resistant to a significant degree. This is attributed to the fact that a thick layer of hydration was developed around the macromolecule, shielding the counter ion and improving the CMITS drilling fluid's salt resistance. Moreover, the introduction of the carboxymethyl group to native starch, combined with gamma irradiation, resulted in a considerable increase in charge number and steric hindrance.

Fig. 2(e) demonstrates the plastic viscosity response when various CMITS concentrations were used at different temperature conditions. The CMITS concentration showed a better response at ambient (70 °F) and higher temperatures (300 °F). The PV at 70 °F without CMITS concentration was 16 cP, while at 300 °F, the PV was 4 cP, which decreased by 75%. On the other hand, the increase up to 2 ppb CMITS concentration resulted in PV of 20 cP and 8 cP at 70 and 300 °F, respectively. This decrease corresponds to 60%. Similarly, the PV value of the 8 ppb CMITS concentration was 29 and 16 cP at 70 and 300 °F, respectively. This is a decrease of 45%, which is the lowest decrease out of the studied samples. In the current work, the lowest value of PV at 300 °F is still acceptable according to API recommendations. It is considered that an optimum PV could enhance the rate of penetration and demand the least pump load. The findings revealed that the modified starch enhanced the plastic viscosity even at higher temperature conditions. The rheological properties of water-based mud are susceptible to higher temperatures; thus, the optimum properties are very important to be obtained under such harsh conditions. In the current study, gamma irradiation and carboxymethylation enhanced starch thermal stability, improving mud rheology at higher temperatures.

The stability of the mud viscosity in the presence of salt was used to determine their salt resistance. Fig. 2(f) presents the combined effect of temperature and salt concentration on the mud viscosity when CMITS (DS 0.66) was added. At 70 °F and without salt concentration, the PV was the highest (29 cP), while it reduced to 25 cP (14% decrease) when the salt concentration increased to 6 M NaCl. However, when the temperature rose to 300 °F, the plastic viscosity reduced to 16 cP and 12 cP with 0 and 6 M NaCl concentrations. This corresponds to a 25% decrease. It shows that the combined effect of salt and temperature degrades the starch's thermal resistance, reducing the overall thermal stability of the mud. Although the highest DS starch performed better, but the longer exposure to the temperature reduced the capabilities of the mud in the presence of excess salts.

### Yield point

The yield point of mud is a very important parameter and, at flowing conditions is determined by the electrochemical

charges in the mud. Chemical additives are generally added into the mud to control yield stress.<sup>32</sup> The yield stress is caused due to the particle–particle interaction. The mud particles might be charged to attract each other, resulting in a high yield point, or they could be similarly charged, leading to a reduced yield point. It is worth mentioning that the yield stress is related to plastic viscosity; thus, almost similar trends have been observed as PV. Fig. 3 shows the effect of different parameters on the yield point. In Fig. 3(a), at 70 °F, without salt and CMITS concentration, the base mud resulted in a YP value of 22 lb/100 ft<sup>2</sup>. For the same temperature, the 2 ppb starch with DS 0.56, 0.64 and 0.66 resulted in the yield stress of 25, 27 and 33 lb/100 ft<sup>2</sup>, respectively. The results show a positive trend with CMITS degree of substitution, increasing 14, 23 and 50% for the studied starches. Similarly, with the increase in starch concentration to 8 ppb, YP was reported as 35, 45 and 51 lb/100 ft<sup>2</sup> for DS 0.56, 0.64 and 0.66, respectively. These correspond to 59, 104 and 132% increase for DS 0.56, 0.64, and 0.66, respectively.

On the other hand, the salt concentration reduced YP values, as shown in Fig. 3(b). It was noted that without salt concentration, the DS 0.56 resulted in the YP value of 35 lb/100 ft<sup>2</sup>. At 0.64 and 0.66, the YP was recorded as 45 and 51 lb/100 ft<sup>2</sup>, showing an increase in the yield stress. When the salt concentration was increased to 6 M NaCl, the YP was reduced to 30, 38 and 44 lb/100 ft<sup>2</sup> for DS 0.56, 0.64 and 0.66, respectively. It shows a 14, 16 and 13% decrease for the studied starches. It is attributed to the damaged network structure between the starch and other mud additives. This damage to the network structure between starch and other additives induced by NaCl in a drilling fluid system can be attributed to multiple factors. The ionic nature of NaCl, leading to the dissociation of sodium ions (Na<sup>+</sup>) and chloride ions (Cl<sup>-</sup>), disrupts the electrostatic interactions between charged functional groups in starch molecules and other additives. This interference weakens cohesive forces within the network structure. Additionally, NaCl induces a “salting out” effect, reducing the solubility of polymers and potentially causing their precipitation or aggregation, further impacting the overall structure of the fluid. Alterations in water activity due to the presence of NaCl influence the hydration and swelling behavior of starch molecules, contributing to changes in the network structure and viscosity of the drilling fluid. Moreover, osmotic effects induced by NaCl result in water movement across the polymer network, exerting stress that disrupts intermolecular interactions within the starch and other additives. Collectively, these mechanisms highlight the intricate ways in which NaCl can detrimentally affect the network structure of a drilling fluid.

Fig. 3(c) demonstrates the combined effect of temperature and degree of substitution on the YP values. When the temperature was raised from 70 °F to 300 °F, the YP declined from 35 to 11 lb/100 ft<sup>2</sup> for DS 0.56. While for DS 0.64, the YP declined from 45 to 17 lb/100 ft<sup>2</sup>. Similarly, the YP was reduced from 51 to 22 lb/100 ft<sup>2</sup> for DS 0.66. The percent decrease for DS 0.56, 0.64 and 0.66 samples were 69%, 62% and 57% respectively. It depicts that the higher DS starch performs superior at high-temperature conditions. Temperature is considered one of



the critical factors which have a more detrimental effect on WBM than OBM. This effect was further increased when the mud was exposed under pressurized conditions for a longer time. It is evident from the results that with an increase in temperature, the overall viscosity of the mud was reduced due to the destruction of the complex network structure developed among the mud additives in the presence of water. It is due to the fact that more water diffuses into the starch granules and causes weakness in the hydrogen bonds in the amorphous region of the starch granules.

The combined effect of starch and salt concentration is shown in Fig. 3(d). As the concentration of starch increases from 2 ppb to 8 ppb, the yield stress also increases, showing a positive trend. For the base fluid, the YP was 27 when the salt concentration was zero. At the same time, at 6 M NaCl concentration, the YP reduced to 24, showing that the biomaterials, including xanthan gum, partially degraded with the addition of salt. When the CMITS 0.66 was added to the mud with a 2 ppb concentration, the YP raised to 32 and 28 lb/100 ft<sup>2</sup> for zero and 6 M NaCl concentration. With a further increase in CMITS concentration to 8 ppb, the YP was raised to 51 and 44 lb/100 ft<sup>2</sup> for 0 and 6 M NaCl concentrations. The results showed that the higher degree CMITS performs better in terms of starch resistance at ambient conditions.

Fig. 3(e) illustrates the effect of temperature and CMITS concentration on yield stress. It shows a decrease from 27 to 6 lb/100 ft<sup>2</sup> for the base sample from 70 to 300 °F. When the concentration of CMITS was 2 ppb, it rose to 32 and 9 lb/100 ft<sup>2</sup> for the same temperatures, which is an increase of 19% and 50% for 70 and 300 °F, respectively. By increasing the CMITS concentration to 8 ppb, the YP increases to 51 and 22 lb/100 ft<sup>2</sup> at 70 and 300 °F, respectively. Compared with the base mud, this is the highest value of the YP, and the percent increase in YP is 89 and 267% for the selected temperatures. From the current results, it is noticed that better performance in terms of YP was obtained both at low and high temperatures when the higher DS CMITS was used as an additive.

The combined effect of salt concentration in the presence of temperature is shown in Fig. 3(f). At 70 and 300 °F, the mud without salt showed the YP values of 51 and 22 lb/100 ft<sup>2</sup>. However, when the salt concentration increased to 6 M NaCl, the YP declined to 44 and 16 lb/100 ft<sup>2</sup> for the studied temperatures. This corresponds to a percent decrease from 14 and 27% for 70 and 300 °F, which shows that still, the mud is capable of carrying cuttings in such harsh conditions of temperature and salt concentration.

### Gel strength

The results of gel strength (both 10 s and 10 min) for the formulated mud are presented in Fig. 4 and 5. Fig. 4(a) shows that the gel strength of the base mud without CMITS concentration was 10 lb/100 ft<sup>2</sup> at 70 °F. When a 2 ppb CMITS 0.56 concentration was added, the GS value increased to 12 lb/100 ft<sup>2</sup>. With a further increase in starch concentration to 8 ppb, the GS (10 s) was recorded as 16 lb/100 ft<sup>2</sup>. Likewise, the CMITS 0.64 and 0.66 were tested for the same temperature conditions,

where the GS was raised to 23 lb/100 ft<sup>2</sup> and 26 lb/100 ft<sup>2</sup> with the 8 ppb CMITS concentration. This is an increase of 60, 130 and 160% for DS 0.56, 0.64 and 0.66 with a dosage of 8 ppb CMITS. From the results, it is observed that the CMITS and the degree of substitution positively affect the gel strength of the mud.

Fig. 4(b) demonstrates the combined effect of salt concentration and degree of substitution on mud's gel strength (10 s). When the salt concentration was zero and CMITS concentration was 8 ppb, the gel strength was observed as 16, 23 and 26 for DS 0.56, 0.64 and 0.66, showing an improvement in the gel strength due to the higher DS starch. However, when the same sample was tested by adding salt with 6 M NaCl concentration, the GS reduced to 14, 19 and 22 lb/100 ft<sup>2</sup> for DS 0.56, 0.64 and 0.66, respectively. It shows a decrease of 12.5%, 17% and 15%. This revealed that the modified starch is more salt-tolerant than the base mud. Although the reduction in the gel strength was observed due to the addition of salt, the changes in the GS values are still acceptable according to the API recommendations.

Similarly, Fig. 4(c) illustrates the effect of the degree of substitution and temperature on the gel strength. At 70 °F, the CMITS starch with DS 0.56, 0.64 and 0.66 resulted in a GS of 13, 23 and 26 lb/100 ft<sup>2</sup>, respectively. While at higher temperatures (300 °F), the same starches showed 3, 7 and 10 lb/100 ft<sup>2</sup>, respectively. It shows that the percentage reduction was 77, 69 and 61% for the studied starches. The gelling property of the mud deteriorated because of the more prolonged exposure to high temperatures. Although there is an overall reduction in the GS, but the minimum reduction was observed when DS 0.66 starch was added to the mud. This shows that the higher DS (0.66) starch can sustain high temperatures compared to the lower DS (0.56) starch and base mud.

Fig. 4(d) shows the combined effect of salt concentration and CMITS loading. It is observed from the results that the base fluid yielded a GS of 14 lb/100 ft<sup>2</sup>, while when the salt concentration was increased to 6 M NaCl, the value was reduced to 8 lb/100 ft<sup>2</sup>. The GS was increased from 14 to 17 when the 2 ppb concentration was added without the salt, while the value was reduced to 11 at 6 M NaCl concentration. At 8 ppb CMITS concentration, the GS was found 26 and 21 lb/100 ft<sup>2</sup> for 0 and 6 M NaCl concentrations. It revealed that the GS has also been affected by salt concentration. But the highest DS (0.66) starch has less reduction than the others. The CMITS concentration also contributed significantly, and the resultant GS values are still acceptable according to the API standards.

Likewise, the effect of CMITS concentration and temperature is shown in Fig. 4(e). At 70 °F, the base fluid shows the GS of 14, while at high temperature (300 °F), it reduced to 3 lb/100 ft<sup>2</sup>. On the other hand, when the starch concentration was raised to 2 ppb, the GS also increased to 16 and 4 at 70 and 300 °F, respectively. With a further increase in starch concentration to 8 ppb, the highest GS was obtained at 26 and 10 for 70 and 300 °F, respectively.

Fig. 4(f) shows the effect of temperature and salt concentration on the GS. At 70 °F and 0 salt concentration, the GS was 26, while at 6 M NaCl concentration, it reduced to 22,





corresponding to a decrease of 15%. When the temperature was increased to 300 °F, the 0 salt concentration showed 10 lb/100 ft<sup>2</sup>, while at 6 M NaCl, it reduced to 9, a decrease of 10%.

From the current findings, it can be concluded that the salt concentration and temperature have a negative impact on the rheological properties of the mud. In contrast, CMITS

concentration and degree of substitution positively influenced the mud properties. Furthermore, when compared with the base fluid, it is noticed that significant improvements have been seen in the rheological properties. From the literature,<sup>33,34</sup> it has been noted that a properly formulated drilling fluid should have a 10 s gel strength greater than at least 4 lb/100 ft<sup>2</sup>, and the

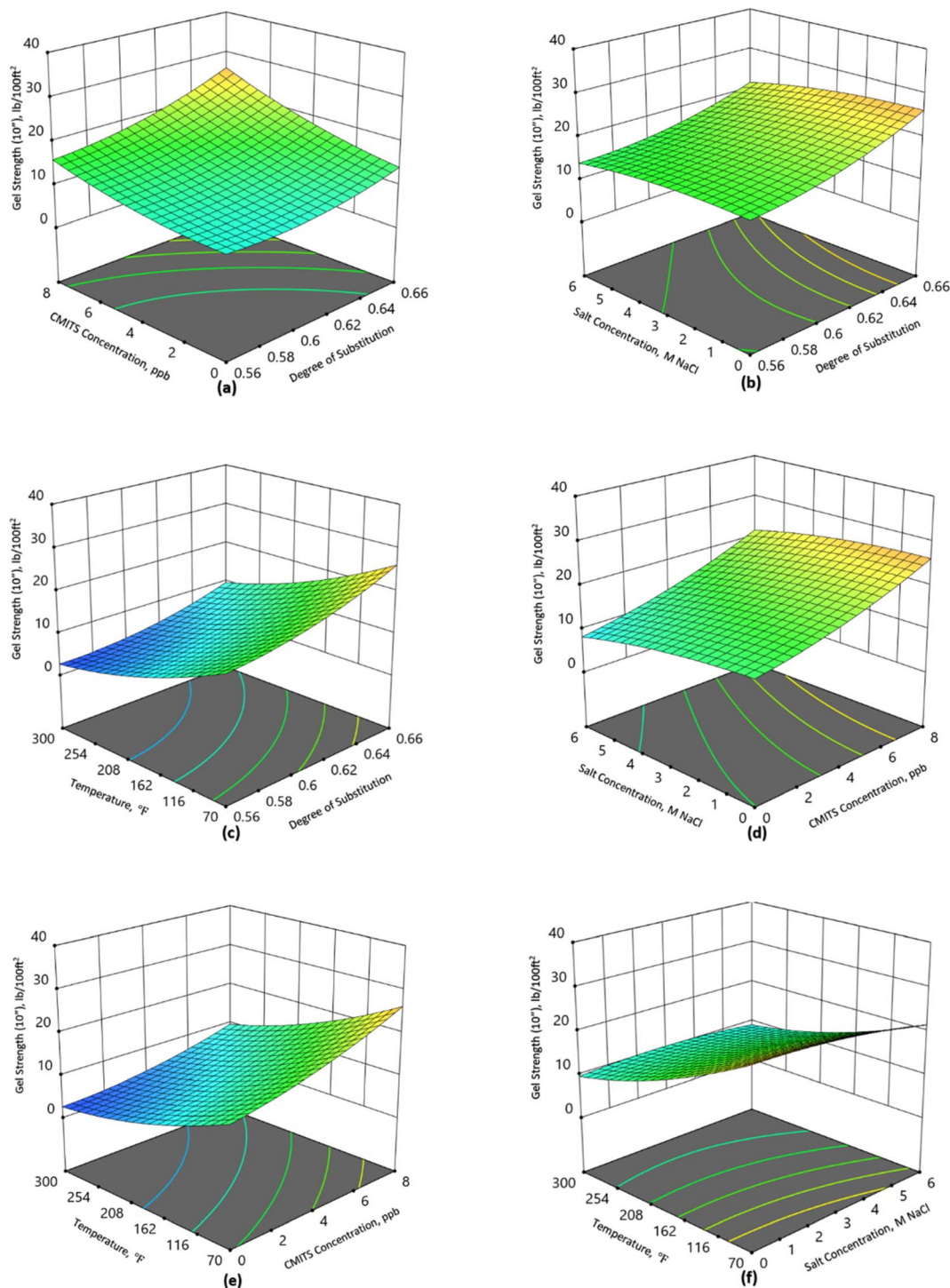


Fig. 4 Influence of (a) DS and CMITS dosage, (b) DS and salt dosage, (c) DS and temperature, (d) CMITS and salt dosage, (e) CMITS dosage and temperature, and (f) salt dosage and temperature on the gel strength ( $10^3$ ).





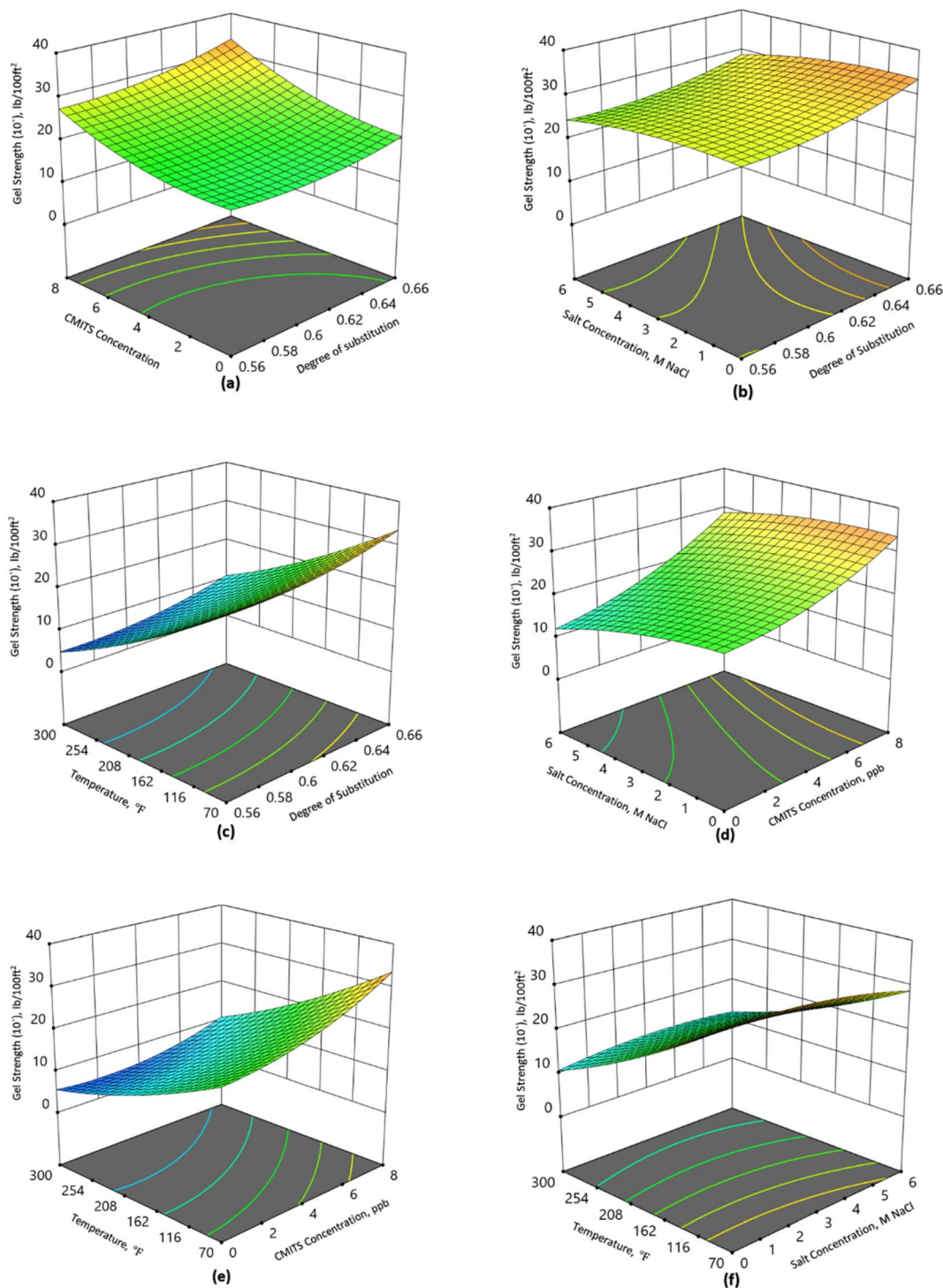


Fig. 5 Influence of (a) DS and CMITS dosage, (b) DS and salt dosage, (c) DS and temperature, (d) CMITS and salt dosage, (e) CMITS dosage and temperature, and (f) salt dosage and temperature on the gel strength ( $10^1$ ).

10 min gel strength should be higher than a minimum of 6 lb/100 ft<sup>2</sup>. The current findings are in agreement with the literature because all the values lie in the range.

Similar to the 10 s gel strength, Fig. 5 generally shows similar trends for 10 minutes gel strength for all the selected parameters.

#### Statistical analysis: analysis of variance

Analysis of Variance (ANOVA) was used as the testing method in the current work. The *F*-test was used to determine the *p*-values. After conducting ANOVA, the *p*-value of all the selected factors was less than 0.05. This implies that an increase in both the CMITS dosage and degree of substitution enhances the selected



properties of the mud. In comparison, the salt concentration and temperature showed a negative trend for the studied samples. Moreover, the salt resistance of the higher DS starch (0.66) was higher as compared to the lower DS starch (0.56).

The following equations (eqn (3)–(6)) have been developed based on the ANOVA analysis by considering the quadratic model, resulting in the highest  $R^2$  and least  $p$ -values.

$$PV = 20.4264 + 1.8A + 4.4B - 1.2C - 6.2D + AB - 0.1AC - 0.1AD - 0.6BC - 0.3BD + 0.1CD + 0.3A^2 - 1.4B^2 + 0.1C^2 - 6.4D^2 \quad (3)$$

$$YP = 20.3 + 3.2A + 6.1B - 1.9C - 10.9D + 3AB - 0.38AC - 1.5AD - 0.95BC - 2.1BD + 0.3CD + 5.1A^2 + 0.8B^2 - 1.65C^2 - 3.7D^2 \quad (4)$$

$$GS (10 \text{ s}) = 5.3 + 2.1A + 3.6B - 0.96C - 5.2D + 1.6AB - 0.7AC - 0.8AD + 0.3BC - 1.3BD + CD + 1.8A^2 + 1.4B^2 - 1.1C^2 + 1.9D^2 \quad (5)$$

$$GS (10 \text{ min}) = 9.86 + 1.6A + 4.5B - 1.4C - 8D + AB - 0.4AC - 0.1AD + BC - 1.9BD + 1.5CD + 1.6A^2 + 2.6B^2 - 1.4C^2 + 1.6 - 1.65D^2 \quad (6)$$

where  $A$ ,  $B$ ,  $C$ , and  $D$  represent the degree of substitution, CMITS concentration, salt concentration, and system temperature, respectively.

From the above equations, it can be observed that the degree of substitution and CMITS concentration have a positive effect. In contrast, the salt dosage and temperature have a negative effect on the overall efficiency of the mud. It has been experimentally confirmed that the mud rheological findings showed that the base mud depicted very unacceptable viscosity at

elevated temperatures. This effect was further worsened when salt was added to the mud. After adding starch with a higher DS value, significant results in terms of rheology improvements were obtained, which is a good indication for borehole cleaning due to proper cuttings transportation. The higher degree of substitution improved the plastic viscosity because more carboxyl groups were added to the starch chain, increasing its solubility and resulting in the gelled fluid. Additionally, better performance was obtained from the highest DS sample when exposed to the elevated temperature for a longer time (16 hours). It confirms that the presence of carboxyl groups enhanced the stereo-hindrance effects and reduced the degree of intramolecular rotation, resulting in easy curling. Thus, the formulated mud samples demonstrated excellent temperature resistance when exposed to higher temperatures for longer times.

Table 2 shows the performance indicators for the developed quadratic models. It is observed that all the parameters showed an  $R^2$  value greater than 0.90, indicating that the models are significant. Similarly, the standard deviation and mean values of the parameters are in the acceptable ranges of the API. Additionally, the predicted  $R^2$  of all the studied parameters reasonably agrees with the adjusted  $R^2$  values (the difference is less than 0.2). The adequate precision that measures the signal-to-noise ratio is found greater than 4, which is desirable. Thus, the developed models can be used to navigate the design space.

### Rheological modelling

It is vital to understand the correlation between shear stress and shear rate in order to analyze the behavior of drilling mud and its potential to suspend and carry drilled cuttings. The development of an appropriate rheological model is essential for

Table 2 Performance indicators of the developed models

Parameters	PV	YP	GS (10 s)	GS (10 min)
$R^2$	0.98	0.95	0.94	0.97
Adjusted $R^2$	0.97	0.93	0.93	0.96
Predicted $R^2$	0.96	0.91	0.90	0.93
Adeq. precision	40.73	29.36	28.99	33.65
Standard deviation	1.37	3.33	1.81	1.90
Mean	14.87	21.60	8.98	13.62
$p$ -value	0.09	0.08	0.12	0.11

Table 4 Selected mud blends for rheological modelling

Sample	DS	CMITS conc.	Salt conc.	Temp.	Desirability
1	0.66	3.150	3.102	70	0.987
2	0.66	8.000	2.889	215	0.824
3	0.66	8.000	4.98	194	0.814
4	0.66	8.000	4.81	208	0.748
5	0.66	7.529	1.41	218	0.739
6	0.66	7.921	4.4	197	0.832
7	0.66	8.000	3.87	204	0.842
8	0.66	3.07	2.44	79	0.961

Table 3 Rheological parameters optimization criteria

Parameter	Goal	Lower limit	Upper limit
Factors	Degree of substitution	Equal to 0.66	0.66
	CMITS concentration	In range	8
	Salt concentration, M NaCl	In range	6
	Temperature, °F	In range	300
Responses	Plastic viscosity, cP	In range	25
	Yield stress, lb/100 ft <sup>2</sup>	In range	35
	Gel strength (10 s), lb/100 ft <sup>2</sup>	In range	25
	Gel strength (10 min), lb/100 ft <sup>2</sup>	In range	30



a comprehensive description of the rheological properties of drilling muds. Drilling fluids are non-Newtonian in nature, showing a non-linear relationship between shear rate and shear

stress. In this work, eight mud blends were selected based on the optimization performed by DOE software. The criteria for optimization were set as given in Table 3. The selected mud

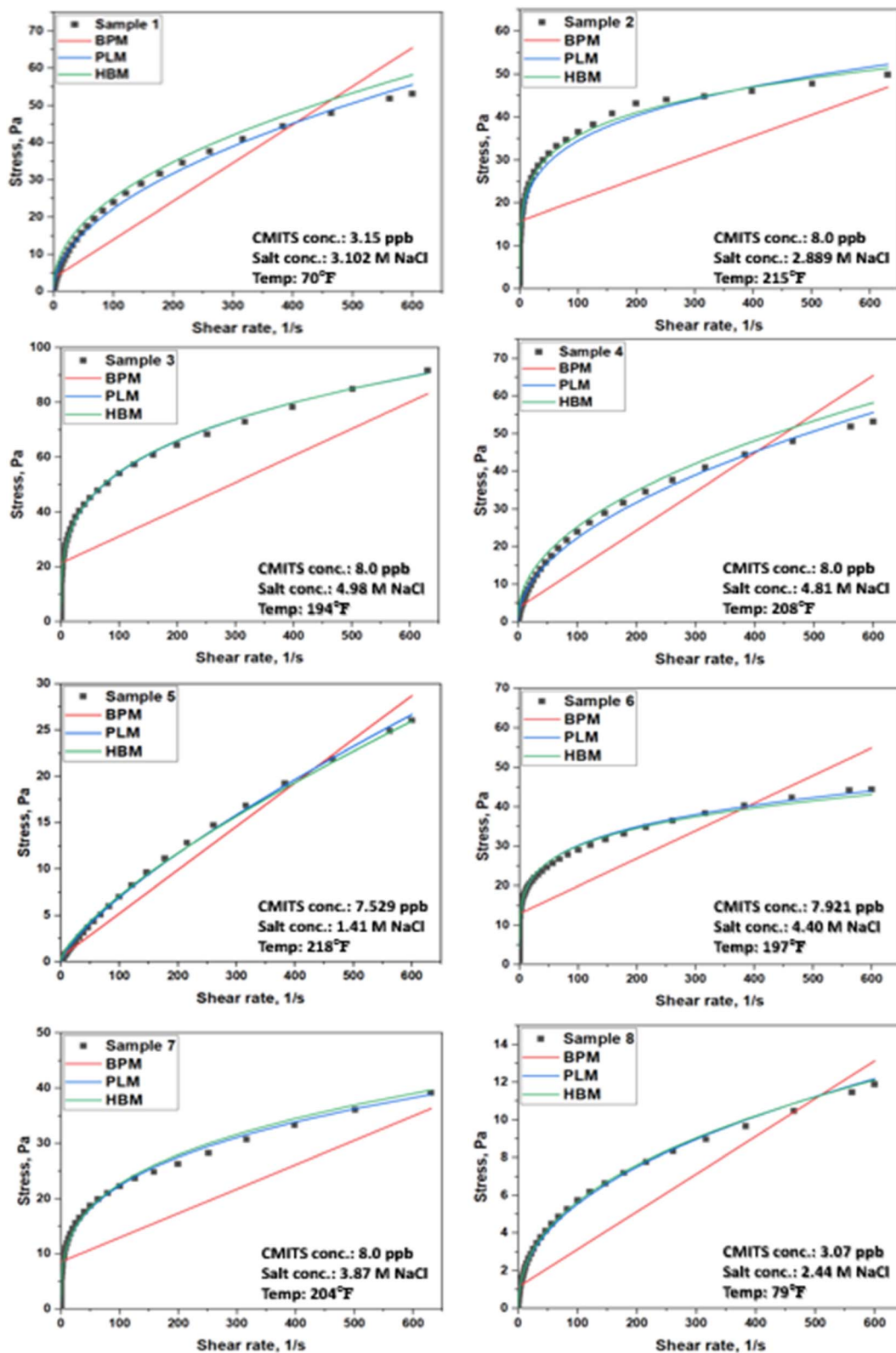


Fig. 6 Rheological model fitting of optimized mud blends with the existing models (based on Table 4).





blends given in Table 4 were tested for their rheological behavior.

All the model's data was plotted using the existing models, including Bingham plastic (BPM), Power-law (PLM), and Hershhal Bulkley (HBM) models, as shown in red, blue, and green lines, respectively. The scattered points (black) show the experimental data obtained from the rheometer.

The rheometer readings in terms of shear stress and shear rate were plotted and presented in Fig. 6. All the tested samples showed a nonlinear relationship between shear stress and shear rate. From the rheograms, it was found that the shear stress values of the mud containing 3.150 ppb CMITS and salt concentration of 3.102 M NaCl at 70 °F showed a model best fitted with the Power-law model. Similarly, the 8 ppb CMITS concentration with a salt concentration of 2.889 M NaCl at 215 ° F showed relatively less stress value. It is due to the effect of temperature and salt concentration. Still, the mud was found stable at this temperature. In sample 3, at 194 °F, the mud containing CMITS concentration 8 ppb and salt concentration 4.98 M NaCl showed higher yield stress than other studied samples. For sample 4, the rheograms showed a similar performance as sample 1 but with a higher stress value. It is due to the addition of more solid particles (CMITS and salts) to the mud. Likewise, in the sample containing CMITS concentration of 7.529 ppb and 1.41 M NaCl at 218 °F, the stress was reduced sharply. In this case, the Bingham plastic model (red) line starts nearly from zero, showing the least yield stress value. In sample 6, the CMITS concentration was 7.921 ppb, and the salt concentration was 4.40 M NaCl, resulting in acceptable values and fitting with the Power-law model. Sample 7 containing 8 ppb CMITS and 3.87 M NaCl concentration was tested at 204 ° F, which also yielded a yield stress value of less than 10 Pa for the Bingham model. Finally, the lowest CMITS dosage of 3.07 ppb and salt concentration of 2.44 M NaCl at 79 °F resulted in a less than 2 Pa yield stress value.

All the studied samples concluded that the temperature and salt concentration affected the starch stability, but still, the values were in an acceptable range. The addition of starch content increased the flow resistance of the mud. Moreover, most of the samples showed the best fitting with the Power-law model except a few, which were best fitted with the Harshal Bulkley model. None of the samples showed fittings with the Bingham Plastic model, and the plots also resulted in an underfit  $R^2$  value ( $<0.5$ ).

Similarly, the relationship between the viscosity and shear rate is shown in Fig. 7. The variation in viscosity is due to the addition of the modified starch and salts. More resistance has been developed as a result of the addition of the particles. Previous research has shown that when the proportion of solids rises, so does the viscosity of the mud. The increased particle frictional interaction resulting from this contact increases the overall viscosity of the system. The studied mud blends showed a shear-thinning behavior for all the cases where the value of  $n$  was less than 1. This value was decreased with an increase in the addition of starch into the mud, which is a positive indication for better cuttings transportation.

The obtained modelling parameters of each model are given in Table 5. The obtained data concluded that all studied samples' data were best fitted with the Power-law model (PLM) with  $R^2$  values higher than 0.98. The flow behavior indices for the samples were less than 1, while the consistency indices varied with the CMITS and salt concentration in the presence of applied temperatures. The value of the flow behavior index was further observed to be reduced with an increase in CMITS concentration. On the other hand, the introduction of starch enhanced the consistency index of the blends. This behavior is very important for better transport capacity. This also indicates that the current mud formulations can transport the cuttings from the bottom hole to the surface without using clayey materials such as bentonite. The  $n$  and  $k$  values for the mud blends showed almost the same shear thinning behavior ( $n < 1$ ).

### Comparative analysis

To compare the current mud formulation with the existing mud formulations in the literature, Table 6 presents rheological properties of various tested materials including XG-SiO<sub>2</sub> nanoparticles, SnO<sub>2</sub> nanoparticles, quadripolymer, drispac, silica

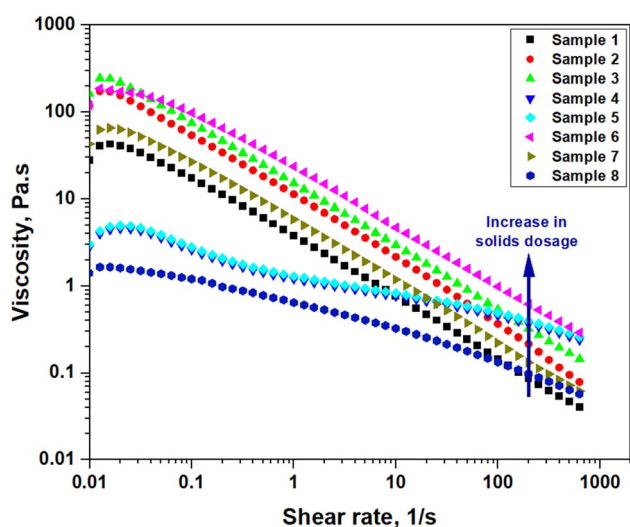


Fig. 7 Shear rate vs. viscosity response of the optimized samples (based on Table 4).

Table 5 Rheological modelling parameters

Sample	Model parameters (Power law model: $\tau = K_r \dot{\gamma}^n$ )	
	$K$	$n$
Sample 1	0.135	0.83
Sample 2	12.2365	0.225214
Sample 3	15.1169	0.278056
Sample 4	2.13	0.51
Sample 5	0.22	0.75
Sample 6	11.49	0.21
Sample 7	5.62	0.3
Sample 8	0.73	0.44



Table 6 Comparison of existing bentonite-free mud formulations with the current mud

Material tested	Rheological properties					Reference
	PV, cP	YP, lb/100 ft <sup>2</sup>	AV, cP	GS		
				GS 10 s	GS 10 min	
XG-SiO <sub>2</sub> nanoparticles	~41	~29	—	~5	~6	35
SnO <sub>2</sub> nanoparticles	~17.8	~28	~31.8	~6.3	~18.3	36
Quadripolymer	16	~19	25	—	—	37
Drispac	17	~15	24	—	—	37
Silica nanoparticles	0.37	8.94	—	—	—	35
Thermo-associating polymer/silica nanocomposite (BFDF + 1%AMS-CGBA)	19	12	25	—	—	38
Thermo-associating polymer/silica nanocomposite (BFDF + 0.5% CGBA)	18	6	21	—	—	38
CMITS	15	20	25	10	12	Current study

nanoparticles, and thermo-associating polymer/silica nanocomposites at different concentrations. The properties include Plastic Viscosity (PV), Yield Point (YP), Apparent Viscosity (AV), Gel Strength (GS) at 10 seconds and 10 minutes. Finally, the current mud formulation results have been included for comparison. The findings indicate that the current mud formulation yields results falling within the recommended ranges outlined by the American Petroleum Institute (API).

## Conclusions

This study extensively examined the complicated rheological behaviors of drilling muds under varying conditions of CMITS concentration, salt content, temperature, and degree of substitution. The investigation showcased the interplay of these factors on mud properties, revealing both positive and negative effects. Enhanced CMITS dosage and degree of substitution contributed positively to mud efficiency and rheological characteristics, leading to improved borehole cleaning potential and better cuttings transportation. The developed quadratic models exhibited strong correlation, as indicated by high  $R^2$  values, and aligned well with API standards for mud performance indicators. The non-Newtonian nature of drilling fluids was evident through nonlinear shear stress–shear rate relationships. Importantly, the study demonstrated the feasibility of mud formulations with heightened CMITS concentrations for effective cuttings transport without relying on conventional clay additives. Overall, these findings offer valuable insights into optimizing drilling mud formulations for enhanced performance in challenging downhole conditions.

## Conflicts of interest

The authors have no conflicts of interest associated with the research, ensuring the integrity and impartiality of the article.

## Acknowledgements

The authors gratefully acknowledge the support of Ministry of Higher Education (MOHE), Malaysia for providing financial assistance under FRGS/1/2020/TK0/UTP/02/3, and Centre of

Graduate Studies (CGS), Universiti Teknologi PETRONAS (UTP) for providing the required facilities to conduct this research.

## References

- H. Wang, H. Huang, W. Bi, G. Ji, B. Zhou and L. Zhuo, *Nat. Gas Ind.*, 2022, **9**, 141–157.
- S. Ghaderi, S. A. Haddadi, S. Davoodi and M. Arjmand, *J. Mol. Liq.*, 2020, **315**, 113707.
- L. Liu, X. Pu, H. Tao, Q. Deng and A. Luo, *RSC Adv.*, 2018, **8**, 11424–11435.
- Y. Wang, B. Jiang, J. Lan, N. Xu, J. Sun and L. Meng, *RSC Adv.*, 2020, **10**, 43204–43212.
- Y. An, G. Jiang, Y. Qi, Q. Ge and L. Zhang, *RSC Adv.*, 2016, **6**, 17246–17255.
- S. Gautam, C. Guria and V. K. Rajak, *J. Pet. Sci. Eng.*, 2022, **213**, 110318.
- K. Liu, H. Du, T. Zheng, H. Liu, M. Zhang, R. Zhang, H. Li, H. Xie, X. Zhang and M. Ma, *Carbohydr. Polym.*, 2021, **259**, 117740.
- L. H. Qitian, D. E. Andrade and A. T. Franco, *Rheol. Acta*, 2022, **61**, 841–855.
- S. Medhi, S. Chowdhury, A. Kumar, D. K. Gupta, Z. Aswal and J. S. Sangwai, *J. Pet. Sci. Eng.*, 2020, **187**, 106826.
- N. D. N. Marques, C. S. D. N. Garcia, L. Y. C. Madruga, M. A. Villetti, M. S. M. De De Filho, E. N. Ito, D. Balaban and R. Carvalho, *J. Renewable Mater.*, 2019, **7**, 139–152.
- J. O. Oseh, M. Norddin, I. Ismail, A. R. Ismail, A. O. Gbadosi and A. Agi, *Appl. Nanosci.*, 2020, **10**, 61–82.
- X. Bai, X. Zhang, Y. Xu and X. Yong, *Starke*, 2021, **73**, 2000151.
- A. Nasiri, M. J. Ameri Shahrabi, M. A. Sharif Nik, H. Heidari and M. Valizadeh, *Pet. Explor. Dev.*, 2018, **45**, 167–171.
- G. Ambuj, *Int. J. Eng. Sci. Comput.*, 2019, **9**, 1–8.
- V. K. Rajak, S. Gautam, K. P. Ajit, R. Kiran and A. Madhumaya, *MAPAN*, 2022, **37**, 665–681.
- X. Yu, L. Chen, Z. Jin and A. Jiao, *J. Mater. Sci.*, 2021, **56**, 11187–11208.
- T. T. V. Tran, N.-N. Nguyen, Q.-D. Nguyen, T.-P. Nguyen and T.-N. Lien, *RSC Adv.*, 2023, **13**, 10005–10014.



- 18 A. A. Sulaimon, S. A. Akintola, M. A. B. Mohd Johari and S. O. Isehunwa, *J. Pet. Explor. Prod.*, 2021, **11**, 203–218.
- 19 D. Soto, O. León, J. Urdaneta, A. Muñoz-Bonilla and M. Fernández-García, *Materials*, 2020, **13**, 2794.
- 20 X. Kong, M. Chen, C. Zhang, Z. Liu, Y. Jin, X. Wang, M. Liu and S. Li, *Molecules*, 2022, **27**, 8936.
- 21 H. Zhong, X. Kong, S. Chen, B. P. Grady and Z. Qiu, *J. Mol. Liq.*, 2021, **325**, 115221.
- 22 Z. Yaoyuan, M. Shuangzheng, C. Jinding, L. Wenming, L. Huayong and W. Guanxiang, *Drilling fluids and completion fluids*, 2019, **36**, 694–699.
- 23 B. L. Lima, N. N. Marques, E. A. Souza and R. C. Balaban, *J. Mol. Liq.*, 2022, **364**, 120023.
- 24 H. Wang, M. Li, J. Wu, P. Yan, G. Liu, K. Sun, Q. Mou and C. Zhang, *J. Polym. Eng.*, 2022, **42**, 163–171.
- 25 A. Arinkoola, T. Salawudeen, K. Salam, M. Jimoh, Z. Atitebi and G. Abidemi, *Iran. J. Chem. Eng.*, 2019, **16**, 39–53.
- 26 D. V. Krishna and M. R. Sankar, *J. Mol. Liq.*, 2023, **388**, 122836.
- 27 I. Ali, M. Ahmad, S. Ridha, C. C. Iferobia and N. Lashari, *Hybrid Adv.*, 2023, **3**, 100071.
- 28 L. Salehnezhad, A. Heydari and M. Fattahi, *J. Mol. Liq.*, 2019, **276**, 417–430.
- 29 M. A. Betiha, G. G. Mohamed, N. A. Negm, M. F. Hussein and H. E. Ahmed, *Arabian J. Chem.*, 2020, **13**, 6201–6220.
- 30 Z. Daud, M. H. Abubakar, M. A. Rosli, M. B. Ridzuan, H. Awang and R. Aliyu, *Int. J. Integr. Eng.*, 2018, **10**, 101.
- 31 K. Song, Q. Wu, M. Li, S. Ren, L. Dong, X. Zhang, T. Lei and Y. Kojima, *Colloids Surf., A*, 2016, **507**, 58–66.
- 32 M. El-Sukkary, F. Ghuiba, G. Sayed, M. Abdou, E. Badr, S. Tawfik and N. Negm, *Egypt. J. Pet.*, 2014, **23**, 7–14.
- 33 X. Gao, H.-Y. Zhong, X.-B. Zhang, A.-L. Chen, Z.-S. Qiu and W.-A. Huang, *Pet. Sci.*, 2021, **18**, 1163–1181.
- 34 H. M. Ahmad, M. S. Kamal and M. A. Al-Harhi, *Appl. Clay Sci.*, 2018, **160**, 226–237.
- 35 J. V. Clavijo, L. J. Roldán, L. Valencia, S. H. Lopera, R. D. Zabala, J. C. Cárdenas, W. Durán, C. A. Franco and F. B. Cortés, *Adv. Nat. Sci.: Nanosci. Nanotechnol.*, 2019, **10**, 045020.
- 36 A. B. M. A. B. Khandaker, N. Ahmed and M. S. Alam, *Pet. Res.*, 2023, DOI: [10.1016/j.ptlrs.2023.03.003](https://doi.org/10.1016/j.ptlrs.2023.03.003).
- 37 J. Wang, M. Chen, X. Li, X. Yin and W. Zheng, *Crystals*, 2022, **12**, 257.
- 38 B. Xie, J. Chen, J. Chen, C. Ma, L. Zhao and A. P. Tchameni, *Geoenergy Sci. Eng.*, 2023, **222**, 211426.

